



Identification of Auxin Activity Like 1, a chemical with weak functions in auxin signaling pathway

Wenbo Li^{1,2} · Haimin Li^{1,2} · Peng Xu^{1,2} · Zhi Xie^{1,2} · Yajin Ye^{2,3} · Lingting Li^{2,3} · Deqiang Li^{1,2} · Yijing Zhang¹ · Laigeng Li¹ · Yang Zhao^{3,4}

Received: 1 February 2018 / Accepted: 17 September 2018 / Published online: 11 October 2018
© Springer Nature B.V. 2018

Abstract

Key message A new synthetic auxin AAL1 with new structure was identified. Different from known auxins, it has weak effects. By AAL1, we found specific amino acids could restore the effects of auxin with similar structure.

Abstract Auxin, one of the most important phytohormones, plays crucial roles in plant growth, development and environmental response. Although many critical regulators have been identified in auxin signaling pathway, some factors, especially those with weak fine-tuning roles, are still yet to be discovered. Through chemical genetic screenings, we identified a small molecule, Auxin Activity Like 1 (AAL1), which can effectively inhibit dark-grown *Arabidopsis thaliana* seedlings. Genetic screening identified AAL1 resistant mutants are also hyposensitive to indole-3-acetic acid (IAA) and 2,4-dichlorophenoxyacetic acid (2,4-D). AAL1 resistant mutants such as *shy2-3c* and *ecr1-2* are well characterized as mutants in auxin signaling pathway. Genetic studies showed that AAL1 functions through auxin receptor Transport Inhibitor Response1 (TIR1) and its functions depend on auxin influx and efflux carriers. Compared with known auxins, AAL1 exhibits relatively weak effects on plant growth, with 20 μ M and 50 μ M IC₅₀ (half growth inhibition chemical concentration) in root and hypocotyl growth respectively. Interestingly, we found the inhibitory effects of AAL1 and IAA could be partially restored by tyrosine and tryptophan respectively, suggesting some amino acids can also affect auxin signaling pathway in a moderate manner. Taken together, our results demonstrate that AAL1 acts through auxin signaling pathway, and AAL1, as a weak auxin activity analog, provides us a tool to study weak genetic interactions in auxin pathway.

Keywords *Arabidopsis* · Chemical genetics · AAL1 · Auxin · Amino acid

Wenbo Li and Haimin Li have contributed equally to this work.

Accession Numbers SHY2/IAA3, AT1G04240; ECR1, AT5G19180; AUX1, AT2G38120; AXR2, AT3G23050; AXR3, AT1G04250; AXR1, AT1G05180; TIR1, AT3G62980; YUC1, AT4G32540; YUC2, AT4G13260; YUC4, AT5G11320; YUC6, AT5G25620; AAL1, F1800-0169.

Electronic supplementary material The online version of this article (<https://doi.org/10.1007/s11103-018-0779-9>) contains supplementary material, which is available to authorized users.

✉ Laigeng Li
lgli@sibs.ac.cn

✉ Yang Zhao
yangzhaotoronto@sina.com

¹ National Key Laboratory of Plant Molecular Genetics, CAS Center for Excellence in Molecular Plant Sciences, Institute of Plant Physiology and Ecology, Chinese Academy of Sciences, Shanghai 200032, China

Introduction

The plant hormone auxin regulates diverse aspects of plant growth, development and stress response (Kazan 2013). Indole-3-acetic acid (IAA) is the main natural auxin that is synthesized from the amino acid tryptophan (Trp) through deamination of Trp to indole-3-pyruvate (IPA) by the TRYPTOPHAN AMINOTRANSFERASE OF ARABIDOPSIS1/TRYPTOPHAN AMINOTRANSFERASE RELATEDs

² University of Chinese Academy of Sciences, Shanghai 200032, China

³ Institute of Plant Physiology and Ecology, Shanghai Institutes for Biological Sciences, Chinese Academy of Sciences, Shanghai 200032, China

⁴ Faculty of Life Science and Technology, Kunming University of Science and Technology, 68 Wenchang Road, Yunnan 650000, China

(TAA1/TARs) family. The YUCCA (YUC) family functions in the conversion of IPA to IAA (Zhao 2010). Polar transport of auxin in higher plants is mediated by AUXIN RESISTANT1/LIKE AUX1 (AUX1/LAX) uptake permeases, ATP Binding Cassette subfamily B (ABCB) transporters and PIN-FORMED (PIN) carrier proteins (Teale et al. 2006; Peer et al. 2011).

Auxin acts as a molecular glue to increase the affinity of Transport Inhibitor Response 1/Auxin signaling F-Box protein (TIR1/AFB) for the Auxin/Indole-3-Acetic Acid (Aux/IAA) protein by extending the protein interaction interface (Tan et al. 2007; Villalobos et al. 2012). The cellular auxin signals are mainly recognized by the TIR1/AFB auxin receptors which prompt the ubiquitin-dependent degradation of Aux/IAA transcriptional repressor family, and cause the de-repression of the auxin response factor (ARF) transcription factors (Reed 2001; Kepinski and Leyser 2005; Li et al. 2016).

Auxin research has been greatly propelled by discovery of numerous compounds regulating auxin metabolism, transport and signaling (Walsh et al. 2006; Simon et al. 2013; Zhao et al. 2003). Synthetic auxins such as 1-naphthaleneacetic acid (NAA) and 2,4-dichlorophenoxyacetic acid (2,4-D) have long been widely used in agriculture and provided as useful tools to study auxin function (Ma and Robert 2014; Enders and Strader 2015). Presently all known synthetic auxins mainly belong to or are derivatives of chemical classes including phenoxy-carboxylic acids, benzoic acids, pyridine carboxylic acids, aromatic carboxylic acids and quinoline carboxylic acids families (Grossmann 2007; Ma and Robert 2014). Due to the variation in structure and chemical characteristics, different auxins may vary in their metabolism, transport and affinity toward TIR1/AFB-Aux/IAA (Estelle 1998; Yang et al. 2006; Hosek et al. 2012; Villalobos et al. 2012). For examples, both IAA and NAA but not 2,4-D are better substrates for the auxin efflux carriers, while both IAA and 2,4-D but not NAA are better substrates for the auxin influx carriers (Estelle 1998). Some auxin precursors could not only be used to study auxin biological function, but also be applied to study auxin biochemical transformation. For example, Indole-3-butyric acid (IBA) has been widely used to study peroxisomes that participate in transforming IBA to IAA (Zolman and Bartel 2004; Zolman et al. 2000, 2008). Zhao et al. identified sirtinol which undergoes a series of biochemical transformations to generate an auxinic compound in *Arabidopsis*. By screening mutants hyposensitive to sirtinol, researchers not only identified components involved in auxin biochemical modification, but also discovered previously unknown protein AtCAND1 which is involved in cycling of the SCF^{TIR1} (Skp1p, Cdc53p/cullin and F-box protein) complex (Dai et al. 2005; Zhao et al. 2003; Cheng et al. 2004). Hence, the discovery of new auxinic compound could be valuable for

dissecting the regulatory relationships of these functionally redundant auxin signaling components.

Due to genetic redundancy and cross talks with other signaling pathways, auxin signal transduction networks are complicated and difficult to be dissected. Plant chemical genetics is a complement of conventional genetics approach for studying plant hormone signaling processes. Researchers have taken advantage of the reversible, tunable and spatiotemporal specific perturbations of active small molecules to identify ABA receptors and jasmonate signaling networks (Park et al. 2009; McCourt and Desveaux 2010; Meesters et al. 2014). Here we report a chemical AAL1 with inhibitory activity on *Arabidopsis* seedling growth. Our genetic and biochemical experiments indicated that AAL1 worked through the auxin receptor TIR1. Different from known auxins, AAL1 does not inhibit apical hook of dark-grown seedlings, and its growth inhibitory effects are relatively weak. We also showed that tyrosine (Tyr) and phenylalanine (Phe) treatments could partially rescue the growth inhibition of AAL1, suggesting AAL1 could be used as a useful tool to identify novel factors with weak functions in auxin signaling pathway.

Results

Identification and characterization of AAL1

To identify molecules that affect plant growth and development, we used 3-day-old dark-grown *Arabidopsis* Columbia (Col-0) seedlings to screen against a synthetic chemical library of 12,000 structurally diverse compounds (Cao et al. 2013; Ye et al. 2016). Col-0 seeds were surface sterilized and grown on 0.5 × MS solid medium containing 100 μM different chemicals. After grown for 3 days under dark conditions, the plant phenotypes were imaged. From our primary screening, about 1700 bioactive chemicals which resulted in any abnormal plant growth phenotypes such as shorter hypocotyl, swollen hypocotyl, shorter root, longer root or poor germination were recorded. 221 chemicals resulting in strong and stable phenotypes were verified in our following confirmation experiments. We then focused on 21 chemicals which strongly inhibits the root growth of dark-grown seedlings. Through our further chemical biological growth examinations, 15 chemicals were confirmed for their strong inhibitory effects on both hypocotyls and roots of the dark-grown seedlings. In this research, we focused on one of these chemicals, N-(4-ethylphenyl)-2-[(2R)-2-methyl-3,5-dioxothiomorpholin-4-yl]acetamide (F1800-0169), which we renamed it as AAL1 (Fig. 1a). AAL1 inhibits the root and hypocotyl growth of dark-grown seedlings in a dose dependent manner (Fig. 1b–d).

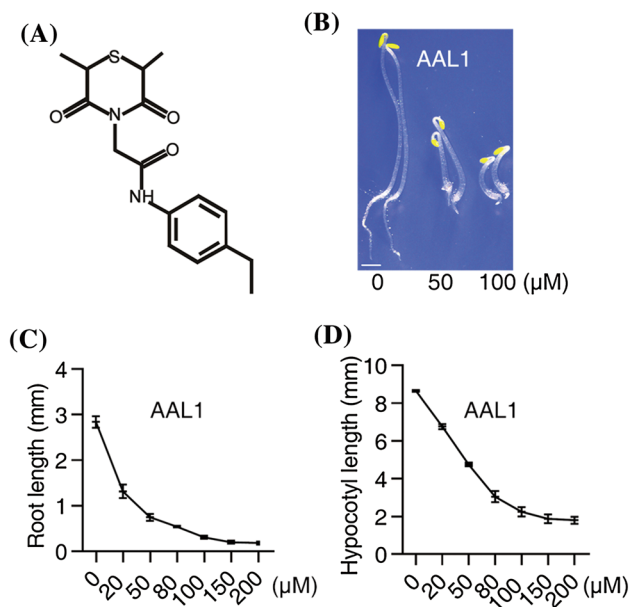


Fig. 1 AAL1 inhibits dark-grown *Arabidopsis* seedlings. **a** The chemical structure of AAL1. **b** The phenotypes of 3-day-old dark-grown Col-0 seedlings on 0.5 × MS solid medium with 0, 50 or 100 μM AAL1. Scale bar, 1 mm. The root **c** and hypocotyl **d** length of dark-grown Col-0 seedlings with different AAL1 concentration. Each dose experiment was repeated three times, and more than 20 seedlings were used every time. The results are the mean length ± SE

AAL1 treated seedlings showed similar phenotypes to that treated by auxin. AAL1 treatments caused dark-grown hypocotyl transverse expansion and inhibited the root growth (Fig. 1b). Under 16-h light/8-h dark (LD) conditions, AAL1 effectively inhibited root elongation in the concentration of 20 μM and inhibited lateral root growth in higher concentrations. It could also increase the adventitious roots number of LD-grown seedlings from approximately one to three (Supplemental Fig. S1). AAL1 showed stronger inhibitory effect on the root growth than the hypocotyl. For the dark-grown seedlings, the half growth inhibition chemical concentration (IC₅₀) for root is about 20 μM and for hypocotyl is about 50 μM (Fig. 1c, d). However, AAL1 does not inhibit the apical hook growth, which is contrary to the phenotype treated with relative low concentration of IAA, NAA and 2,4-D (Supplemental Fig. S3). AAL1 only could inhibit apical hook in a very high concentration, such as 180 μM (Supplemental Fig. S1).

We also examined biological functions of AAL1 structure analogues in the chemical library. We found that two analogues, F1800-0061 and F1800-0093 showed similar but weaker activity compared to AAL1 (Supplemental Fig. S2). This suggests AAL1 related chemicals also have similar functions on plant growth.

Identification and genetic characterization of AAL1-resistant mutants

To determine the modes-of-action of AAL1, AAL1 hypersensitive mutants were screened using 100,000 ethyl methane sulfonate (EMS)-mutagenized M2 seeds of Columbia (Col-0). EMS seeds were grown on 0.5 × MS solid medium with 100 μM AAL1 in the dark for 3 days. Mutants showed longer root or hypocotyl compared with the wild type were selected. We obtained 195 mutants in the first screening. Seven of them failed to survive after being moved to soil and 43 of them were verified as true AAL1 hypersensitive mutants in the next generations.

We found that the phenotypes treated by AAL1 were similar to that treated by auxin (Supplemental Fig. S3). Then we tested the sensitivity of these AAL1 resistant mutants to 1 μM IAA for root growth phenotype under LD condition. Our results showed that all these AAL1 resistant mutants were resistant to IAA. Similarly, AAL1 resistant mutants are also hypersensitive to 2,4-D when grown in the dark-grown condition. These results indicated AAL1 may act as an auxinic compound.

One of the dominant AAL1 resistant mutants showed dwarf phenotypes under LD conditions and was designated as *shy2-3c* (Supplemental Fig. S4). *shy2-3c* was also resistant to the root growth inhibition when treated with 2,4-D (Fig. 2b, c). A follow up genetic analysis using F2 population of *shy2-3c* (c means Col-0 background) and Landsberg erecta (Ler) showed that AAL1 resistance is determined by a single dominant locus. Using 200 AAL1-sensitive F2 lines, *shy2-3c* was mapped to an approximate 229 kb region between the molecular markers 1-AC003027-0319 and 1-AC000104-0395 on chromosome 1 of *Arabidopsis* (Fig. 2a). Auxin-associated genes *SHORT HYPOCOTYL 2* (*SHY2/IAA3*) and *AUXIN RESISTANT 3* (*AXR3*) are located in this region and their mutants showed similar phenotypes with *shy2-3c* (Rouse et al. 1998; Tian et al. 2002). We then sequenced the genomic DNA of *SHY2/IAA3* and *AXR3* of *shy2-3c*, and the results showed the mutant harbors the same mutation as that of the mutant *shy2-3* in Ler background (Tian and Reed 1999). Therefore, these results indicate that AUX/IAAs may play an important role in AAL1-mediated plant growth inhibition.

AAL1 acts through the auxin signal transduction pathway

To further explore how AAL1 acts associated with auxin signaling pathway, we assayed the AAL1 sensitivities of two reported AUX/IAA gain-of-function mutants, *axr2-1* and *axr3-1* (Nagpal et al. 2000; Ouellet et al. 2001). The results showed these mutants were resistant to AAL1 (Fig. 2c). We then analyzed the sensitivities of *arf* mutants including

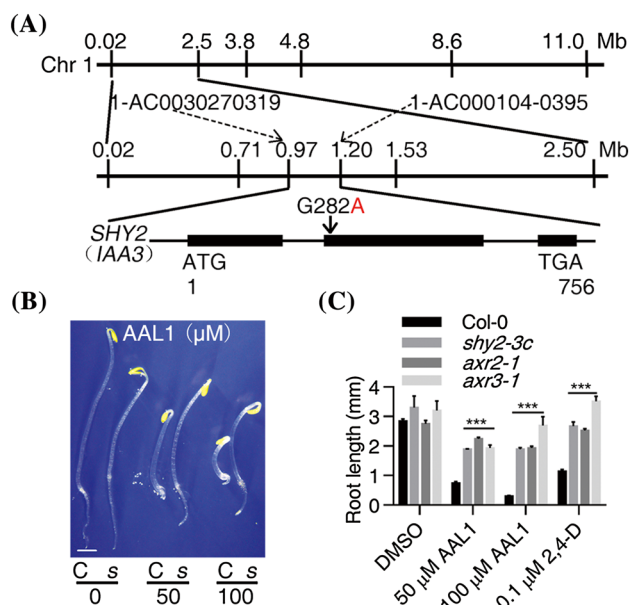


Fig. 2 AUX/IAAs mutants are resistant to AAL1. **a** Schematic procedures of the map-based cloning and sequencing of AAL1 resistant mutant *shy2-3c*. Dashed arrows indicate names of the two closest flanking markers from *shy2-3* locus. **b** The phenotypes of 3-day-old dark-grown Col-0 (C) and *shy2-3c* (s) seedlings grown on 0.5 × MS solid medium with 0, 50 and 100 μM AAL1. Scale bar, 1 mm. **c** The effects of 1% DMSO (DMSO), 0.1 μM 2,4-D, 50 or 100 μM AAL1 on the root growth of Col-0, *shy2-3c*, *axr2-1* and *axr3-1* seedlings grown in dark for 3 days. Each treatment experiment was repeated three times, and more than 20 seedlings were used every time. The results shown are the mean length ± SE. ***P < 0.0001 (two-tailed Student's t-test) indicates a significant difference of the root length compared to Col-0

arf7-1, *arf6/8*, *arf10/16*, *arf17* and *arf19-1* to AAL1 (Ye et al. 2016; Liu et al. 2013; Okushima et al. 2005). The results showed that they were all resistant to AAL1 treatments under dark-grown conditions (Supplemental Fig. S5). Then we used *DR5::GUS* reporter system to test how AAL1 possibly affect auxin signaling pathway. AAL1 treatments resulted in significantly increased expression of *DR5::GUS* in hypocotyls and roots (Supplemental Fig. S5). These results suggest AAL1 activates auxin pathway possibly through AUX/IAAs and ARFs.

Next, we chose auxin receptor mutant *tir1-1* (Ruegger et al. 1998) and auxin biosynthesis quadruple mutant *yuc1/2/4/6* (Cheng et al. 2006) to test how they respond to AAL1 treatment. The results showed *tir1-1* was resistant to AAL1 treatment both in dark and light conditions (Fig. 3a; Supplemental Fig. S1 and S5). However, resistance of *yuc1/2/4/6* to AAL1 was not significant in dark-grown conditions. Also, expression levels of some auxin biosynthesis genes such as *TAA1* and *CYP7B2* (Liu et al. 2017) was not changed under AAL1 treatment (Supplemental Fig. S5). These results indicated that AAL1 may target

auxin signaling pathway rather than auxin biosynthesis. We also examined the effects of AAL1 on the hypocotyl growth of seedlings under light-grown conditions. Col-0 and *yuc1/2/4/6* seeds were grown on 0.5 × MS solid medium (plus 1% sucrose) with 0, 10, and 20 μM AAL1 for 6 days under LD conditions. The results showed that AAL1 can enhance the hypocotyl elongation in both Col-0 and *yuc1/2/4/6* (Fig. 3b, c).

We further used the DII-VENUS transgenic lines to assay how AAL1 treatment affects cellular auxin signal transduction (Ye et al. 2016). The results indicated that 50 μM AAL1 treatments led to a rapid degradation of the DII-VENUS fluorescent signal within 0.5 h in plant cells. However, when compared with the treatments of 0.5 μM 2,4-D and 5 μM IAA, the effects of 50 μM AAL1 treatments on the DII-VENUS fluorescent signal degradation is weak (Fig. 3e and Supplemental Fig. S6). These results suggest that AAL1 is involved in auxin signaling pathway likely through TIR1-mediated protein degradation. Consistent with AAL1 functions in auxin signaling pathway, the expression of downstream auxin response genes *ARF19*, *IAA2* and *GH3.3* (Lavy et al. 2016) were dramatically increased after 0.5 h AAL1 treatment (Fig. 3d).

We also carried out the molecule docking to study the relationship between AAL1 and auxin receptor. Using IAA-TIR1 and 2,4-D-TIR1 as simulations, the molecular docking results are comparable to real interaction conformation from structure researches (Supplemental Fig. S7) (Tan et al. 2007; Villalobos et al. 2012), suggesting the reliability of our molecule docking system. Then we analyzed the interaction of AAL1 and auxin receptor TIR1. The docking results showed that aldehyde groups of AAL1 could form hydrogen bonds with Arg403 and Ser438 of TIR1 (Fig. 4). The binding energy of the top 10 predicted best binding conformers of AAL1 is about −7.7 Kcal/mol, and the *K_i* is from 2.61 μM to about 10 μM. In our docking system, IAA and 2,4-D's silico docking *K_i* is from about 1 μM to about 10 μM, which is similar with that of AAL1. These results suggest AAL1 is energetically favorable to bind to TIR1-IAAs complex to exert its biological function.

AAL1 induces aggravated apical hook phenotype

In order to further study the action of AAL1 and the difference between AAL1 and known auxins, we focused on a weak recessive AAL1 hyposensitive mutant named *ecr1-2* identified in this study. The mutant has weak resistance to AAL1, but shows stronger resistance to 2,4-D (Fig. 5a, b). It is intriguing that *ecr1-2* has exaggerated apical hook phenotype in dark. AAL1 aggravates the apical hook phenotype while 2,4-D inhibits the apical hook. The responsible mutation of *ecr1-2* was mapped to an approximately 318 kb region between the molecular markers 5-AC068655-2333

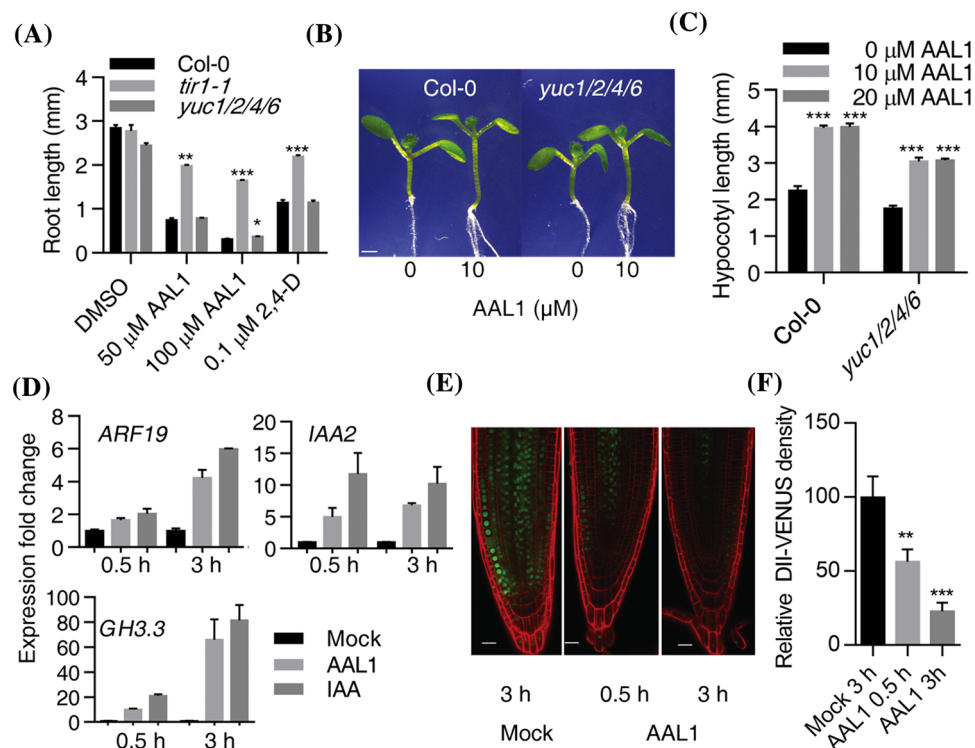


Fig. 3 AAL1 acts through auxin receptor. **a** The root length of 3-day-old dark-grown seedlings of Col-0, *tir1-1* and *yuc1 yuc2 yuc4 yuc6* treated with 1% DMSO, 0.1 μM 2,4-D, 50 and 100 μM AAL1. Scale bar, 1 mm. **b** Phenotypes of 6-day-old light-grown Col-0 and *yuc1 yuc2 yuc4 yuc6* seedlings treated with 0 or 10 μM AAL1. Scale bar, 1 mm. **c** Hypocotyl lengths of Col-0 and *yuc1 yuc2 yuc4 yuc6* seedlings in **(b)**. **d** The relative gene expression levels of *ARF19*, *IAA2* and *GH3.3* affected by AAL1 and IAA. 3-day-old dark-grown Col-0 seedlings were dipped in 0.5 x MS media with the mock (1% DMSO), 50 μM AAL1 or 10 μM IAA for 0.5 h or 3 h. The results

shown are the mean gene expression level \pm SE, $n=3$. **e** AAL1 promotes the degradation of DII-VENUS signal. The 5-day-old light-grown *DII-VENUS* transgenic seedlings were dipped in 0.5 x MS liquid media with the mock (1% DMSO) or 50 μM AAL1 for 0.5 h or 3 h. Scale bar, 20 μm . In **a** and **c**, each experiment was repeated three times, and more than 20 seedlings were used every time. The results shown are the mean length \pm SE. * $P<0.05$, ** $P<0.01$, *** $P<0.0001$ (two-tailed Student's t-test) indicate a significant difference of mutant compared to Col-0

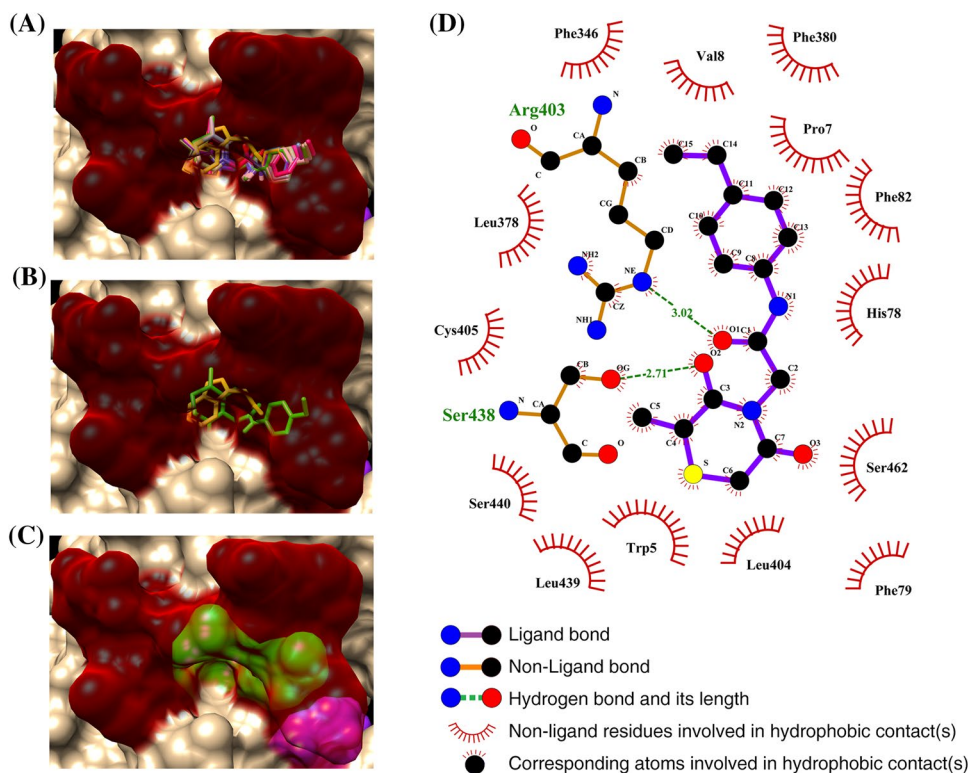
and 5-AF296838-2451 (Supplemental Fig. S8a). Fine mapping and sequence analysis revealed that a glutamic acid to asparagine substitution occurred at the position of the 182th amino acid of the *E1 C-TERMINAL RELATED 1* (*ECR1*) protein. *ECR1* encodes a subunit of ubiquitin-dependent degradation machinery (Del Pozo et al. 2002). The mutant *ecr1-1* has been reported to be resistant to an auxin-like compound indole-3-propionic acid (IPrA) (Woodward et al. 2007). Our further assays confirmed that *ECR1* driven by its own promoter could complement both AAL1 and 2,4-D resistant phenotype of *ecr1-2* (Fig. 5b). Multi-alignment of *ECR1* in common model organisms including *Arabidopsis thaliana*, *Oryza sativa*, *Homo sapiens*, *Mus musculus*, *Danio rerio*, *Drosophila melanogaster*, *C. elegans* and *Saccharomyces cerevisiae* showed the mutation position and its flanking sequences of *ecr1-2* were more conserved than that of previously reported *ecr1-1* mutant (Supplemental Fig. S8b).

AUXIN RESISTANT 1 (*AXR1*), a subunit of the RUB1 activating enzyme, (Leyser et al. 1993), forms the RUB/

NEDD8 activating enzyme complex with *ECR1* to regulate protein degradation including auxin co-receptor complex (Del Pozo et al. 2002). We therefore studied how AAL1 affected *axr1-3* (Leyser et al. 1993). The result showed *axr1-3* was resistant to AAL1. It is interesting that AAL1 treatments also aggravate the apical hook of *axr1-3* in dark (Supplemental Fig. S9b). We also analyzed other known auxin resistant mutants, and found that *axr2-1*, *axr3-1*, *arf6/8* and *arf17* also had the similar phenotype (Supplemental Fig. S5a). AAL1 aggravates but 2,4-D inhibits the apical hook phenotype.

It is well-known that the exaggerated apical hook is related to ethylene signaling. Then we assayed how ACC synthase (ACS) inhibitor AVG and ethylene signaling pathway inhibitor Ag^+ affect the AAL1 treated seedlings. The results showed both AVG and Ag^+ treatments partially restored the exaggerated apical hook of *ecr1-2* (Fig. 5c, Supplemental Fig. S10). As Ag^+ could promote IAA efflux independent ethylene pathway (Strader et al. 2009) and AVG

Fig. 4 Molecule docking analysis of AAL1 and TIR1-IAA7 complex interaction. **a–c** AutoDock4 results were visualized by Chimera. IAA7 degron peptide was shown in red. TIR1 was shown in brown. Inositol hexakisphosphate was shown in purple. Top 10 predicted best binding conformers of AAL1 by AutoDock4 were shown as colorful sticks in **a**. The predicted best binding conformer of AAL1 was shown in green in **b** and **c**. The ligand shown as brown stick in **b** was natural auxin IAA. **d** The 2D docking conformation of the predicted best binding conformer of AAL1 and TIR1-IAA7



could also inhibit members of the TAA1 family of auxin biosynthesis enzymes (Soeno et al. 2010), we then used ethylene pathway mutants. Ethylene resistant mutant *etr1-1* and *ein2-5* are hyposensitive to AAL1 treatments (Fig. 5), indicating the ethylene pathway interaction with AAL1. Because *ein2-5* is completely insensitive to ethylene but partially resistant to AAL1, it is less likely AAL1 directly targets ethylene signaling pathway. We further assayed how Ag^+ and AVG treatments affected auxin function. Our results showed that both Ag^+ and AVG treatments restored the hypocotyl but not root growth inhibitions by IAA, NAA and 2,4-D (Supplemental Fig. S10d).

We then compared the apical hook phenotypes treated by IAA and NAA, and found that none of them showed the aggravated apical hook phenotype. IAA and NAA treatments slightly alleviate the apical hook phenotype at their IC_{50} concentrations for the hypocotyl growth inhibition. 2,4-D treatments strongly reduce the apical hook phenotype at rather low concentrations when compared with IAA and NAA (Supplemental Fig. S10d). Therefore, although AAL1 exhibit similar functions in root inhibition, it differs with from known auxins in promoting seedling apical hook phenotype.

AAL1 functions depend on auxin transporter system

Polarized transport in *planta* is necessary for auxin functions. Through EMS screening, we identified a recessive

mutant *aux1-439aa* that was hyposensitive to AAL1 (Fig. 6a–c). Interestingly, it was mapped to an approximately 260 kb region between the molecular markers 2-AC004684-8036 and 2-AC004683-8170, where the auxin permease gene *AUX1* is located (Supplemental Fig. S11a). Genomic DNA sequencing at *AUX1* locus showed that the 3158th nucleotide of *aux1-439aa* was mutated from G to A, resulting in the mutation from Gly to Glu in the 439th amino acid of *aux1-439aa*. *aux1-439aa* showed abnormal gravitropism phenotype (Supplemental Fig. S11d) as the known mutant *aux1-22* did (Swarup et al. 2004). *aux1-439aa* is also resistant to 2,4-D treatment, similar to *AUX1* loss-of-function mutants *aux1-7* (Marchant et al. 1999). To further elucidate that *AUX1* is essential for AAL1 function, we tested the gravitropism of all AAL1 resistant mutants acquired in this study. Another 5 AAL1 resistant mutants with abnormal gravitropism phenotype were uncovered. Genomic DNA sequencing showed all of them had mutations in *aux1* alleles (Supplemental Fig. S11b).

Among these 6 *aux1* mutant alleles acquired in the study, the mutation of *aux1-439aa*^{Gly439Glu} was reported previously as *aux1-105*^{Gly439Arg} in Wassilewskija (WS) accession, *aux1-92aa*^{Trp92Stop} mutation was reported in RLD accession (Swarup et al. 2004). 4 *aux1* mutant alleles, *aux1-87aa*^{Gly87Asp}, *aux1-143aa*^{Cys143Tyr}, *aux1-196aa*^{Trp196Stop}, and *aux1-467aa*^{Cys467Tyr} are firstly reported in this research. These independent genetic

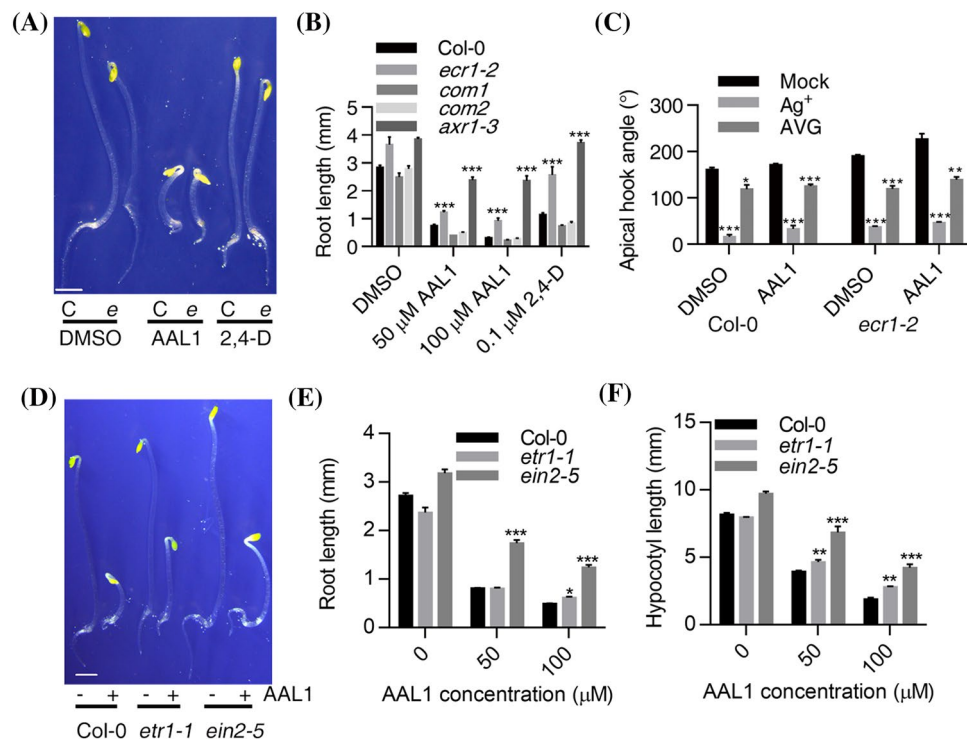


Fig. 5 Characterization and identification of a weak AAL1 hypersensitive mutant *ecr1-2*. **a** The phenotypes of 3-day-old dark-grown Col-0 (C) and *ecr1-2* (e) with 1% DMSO, 100 μ M AAL or 0.1 μ M 2,4-D. Scale bar, 1 mm. **b** The root length of seedlings of Col-0, *ecr1-2* and its genetic complementary lines *com1* and *com2* as well as *axr1-3* grown in dark. **c** The apical hook angles of 3-day-old dark-grown Col-0 and *ecr1-2* seedlings on 0.5 \times MS solid medium with none (mock), 100 μ M Ag^+ or 10 μ M AVG coupled with or without 100 μ M AAL1. * P <0.05, ** P <0.01, *** P <0.0001 (two-tailed

Student's t-test) indicate a significant difference between a treated group and the mock. **d** The phenotypes of 3-day-old dark-grown Col-0, *etr1-1* and *ein2-5* seedlings on 0.5 \times MS solid medium with DMSO or 100 μ M AAL1. Root **e** and hypocotyl **f** length of seedlings as shown in (**d**). In (**b**), (**c**), (**e**) and (**f**), the results shown are the mean length \pm SE. Each experiment was repeated three times, and more than 20 seedlings were used every time. ** P <0.01 and *** P <0.0001 (two-tailed Student's t-test) indicate a significant difference between a mutant and Col-0

mutations suggest that AUX1 is required for AAL1 function, and AAL1 may be transported by auxin influx carrier AUX1.

Since AAL1 works depending on auxin influx carrier AUX1, we also explored whether the transport of AAL1 *in planta* could also be mediated by auxin efflux carriers. We treated dark-grown *Arabidopsis* seedlings with AAL1 and an auxin efflux inhibitor 1-*N*-naphthylphthalamic acid (NPA) (Muday and Murphy 2002). Our results showed 0.05 μ M NPA could partially restore the growth inhibitory effects of AAL1 on plants (Fig. 6d–f). We also assayed whether NPA could restore the inhibitory effects of IAA, NAA and 2,4-D on plants. The results showed that the inhibitory effects of NAA on root growth could also be slightly restored by NPA (Fig. 6e, f). Taken together, the biological functions of AAL1 are dependent on both auxin influx and efflux transporters.

Tyr and Phe could partially restore the effects of AAL1

Structure comparison showed indolyl group of IAA and naphthyl group of NAA were absent in AAL1 molecule.

However, AAL1 has a benzene ring that is similar to 2,4-D. Also the structure of 2,4-D was similar to tyrosine, rather than the auxin biosynthesis precursor tryptophan (Supplemental Fig. S12). Because the auxinic effects of AAL1 are weaker than that of these known auxins such as IAA and 2,4-D, we attempted to use AAL1 to identify regulatory factors with weak functions in auxin pathway.

It was reported that specific amino acids could affect auxin pathway. Trp is the precursor of IAA (Zhao 2010). Some amino acids could conjugate with IAA to affect auxin pathway (Staswick et al. 2005; Staswick 2009). As known auxins induce strong phenotypes on seedling, it is difficult to study how amino acids can affect auxin function. Therefore, we assayed the effects of different amino acids including Tyr, Phe, Trp, histidine (His) and leucine (Leu) on dark-grown seedlings in the presence of AAL1. Our results showed that Tyr and Phe rather than Trp, could noticeably reverse AAL1-induced growth inhibition on plants (Fig. 7a–c). We also tested whether these amino acids could also restore the inhibitory effects of IAA, NAA and 2,4-D. The results showed the inhibitory effect of high

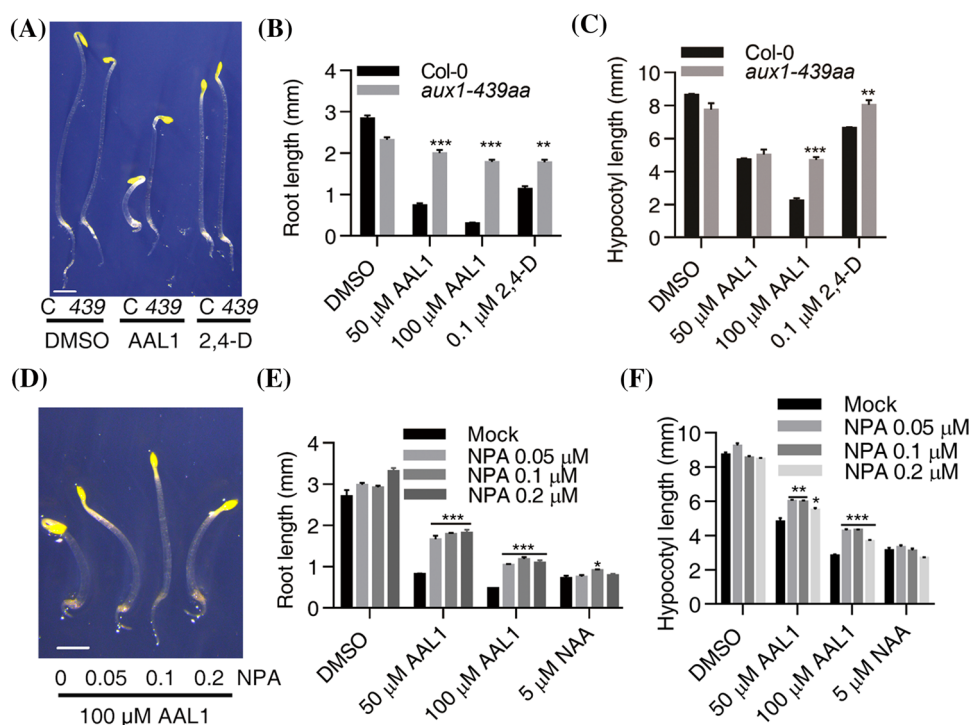


Fig. 6 AAL1 works depending on auxin transport system. **a** The phenotypes of 3-day-old dark-grown Col-0 (C) and *aux1-439aa* (439) with 1% DMSO, 100 μM AAL or 0.1 μM 2,4-D. Scale bar, 1 mm. Root **b** and hypocotyl length **c** of seedlings as shown in **a**. **P < 0.01 and ***P < 0.0001 (two-tailed Student's t-test) indicate a significant difference between *aux1-439aa* and Col-0. **d** 3-day-old dark-grown Col-0 seedlings on 0.5xMS solid medium with none, 0.05, 0.1, or

0.2 μM NPA coupled with 100 μM AAL1. Scale bar, 1 mm. Root **e** and hypocotyl **f** length of seedlings as shown in **d**. The results shown are the mean length ± SE. *P < 0.05, **P < 0.01 and ***P < 0.0001 (two-tailed Student's t-test) indicate a significant difference between a NPA treated group and the mock group. Each experiment was repeated three times, and more than 20 seedlings were used every time

concentration 2,4-D on hypocotyl growth could only be restored by Tyr and Phe. Trp could also slightly restore the effects of 2,4-D with a high concentration (Supplemental Fig. S13a,b). It is likely that effects of known auxins are too strong to be restored by specific amino acids under dark-grown condition.

Under light grown condition, 200 μM Tyr and Phe could also restore the inhibition of 50 μM AAL1 (Fig. 7d, e). Similar results were obtained with other concentrations of AAL1 and Tyr (Supplemental Fig. S13c, d). For 2,4-D, the results are similar to the situation under dark grown condition. 400 μM Tyr or Phe could partially restore the inhibition of 0.05 μM 2,4-D. 200 μM Trp could also slightly restore but the effects are weak (Fig. 7e; Supplemental Fig. S13e, f). Because the structure of IAA is similar to Trp, we tested whether Trp can affect IAA action (Supplemental Fig. S13). IAA inhibits root growth of light-grown seedling at the concentration of 0.3 μM (Fig. 7d, e). 200 μM Trp could partially restore the inhibition of IAA, whereas Tyr and Phe could not. Thus, these evidences suggest that actions of auxins could be affected by specific amino acids that with similar structures.

Discussion

Conventional genetics approaches have led to the identification of many molecular players involved in auxin signaling network. However, genetic redundancy and complicated regulatory networks pose tremendous challenges for studying auxin pathway. Plant chemical genetics approaches use small bioactive chemicals to interrogate cellular networks and have provided new tools for these questions (Zhao et al. 2007; Ye et al. 2017).

In this study, by chemical genetics approaches, we identified a bioactive small molecule AAL1, which acts through auxin signaling pathway. The structure of AAL1 is composed of an ethylphenyl moiety and a dioxithiomorpholin moiety linked by an amide (Fig. 1a). Its structure shares no significant similarity with any reported auxins (Grossmann 2007). AAL1 could induce similar phenotypes as known auxins. High concentrations of AAL1 inhibit the root and hypocotyl growth of dark-grown *Arabidopsis* seedlings. Light-grown primary roots are also inhibited by AAL1 (Fig. 1; Supplemental Fig. S1).

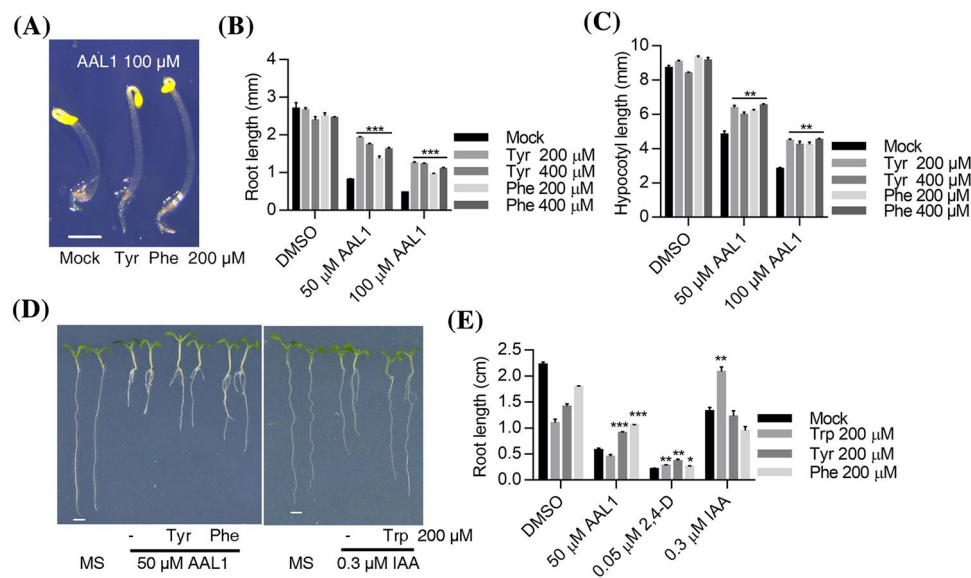


Fig. 7 Tyr and Phe could partially restore the effects of AAL1 and Trp could restore the effects of IAA. **a** The phenotypes of Col-0 seedlings grown in dark on $0.5 \times$ MS solid medium with none (the mock), 200 μM Tyr or Phe coupled with 100 μM AAL1. Root **b** and hypocotyl **c** length of Col-0 seedlings as shown in **a**. **d** The phenotypes of 6-day-old light-grown Col-0 seedlings grown in dark on $0.5 \times$ MS solid medium with none (the mock), 200 μM amino acid Tyr, Phe or

Trp coupled with 50 μM AAL1 or 0.3 μM IAA. **e** The root length of Col-0 seedlings as shown in **d**. Each experiment was repeated three times, and more than 20 seedlings were used every time. The results shown are the mean length \pm SE. ** $P < 0.05$, *** $P < 0.01$ and **** $P < 0.0001$ (two-tailed Student's *t*-test) indicate a significant difference between the amino acid treated group and the mock

With similar mutant screening strategy (Zhao et al. 2003), we acquired many mutants that are resistant to AAL1 treatment. However, these mutants are also hypersensitive to IAA and 2,4-D. Some AAL1 resistant mutants including *shy2-3c* and *ecr1-2* are well characterized regulator in auxin signaling pathway (Fig. 2). Mutant of auxin receptor *tir1-1* is also resistant to AAL1, suggesting AAL1 and auxins act through convergent pathways. This hypothesis is also supported by several other evidences such as response of auxin signal genes and degradation of DII-VENUS signals to AAL1 treatment, as well as molecular docking results (Figs. 3, 4). We did not discover any mutant encoding such enzyme as hydrolase involving in the biochemical modification of AAL1, suggesting AAL1 functions in a different way from the chemical sirtinol (Dai et al. 2005; Zhao et al. 2003). Liquid chromatography–mass spectrometry (LC-MS) analyses of AAL1 treated plants additionally revealed the accumulation of a chemical with the same mass and retention time of AAL1 in seedlings (Supplemental Fig. S14), indicating that AAL1 may work mainly with the un-modified status. This observation is also consistent with our real time expression and molecule docking analysis results (Fig. 3).

Besides the structure difference, we found other differences between AAL1 and known auxins such as IAA, NAA and 2,4-D. First, AAL1 shows a weaker effect. Compared with 5 μM IAA/NAA, 50 μM AAL1 is required to inhibit root and hypocotyl growth under dark grown condition,

while less than 0.5 μM 2,4-D could completely inhibit dark-grown seedling root growth (Supplemental Fig. S3). Under light grown condition, more AAL1 is also needed than IAA to inhibit primary root growth (Fig. 7d). This weak effects might not be caused by weak binding affinities to auxin receptors because we found the docking *K_i* of AAL1 was similar to that of known auxins. Other factors might affect AAL1's efficiency in vivo, for example absorption efficiency and translocation efficiency.

Another difference between AAL1 and known auxins is the apical hook phenotype of dark-grown hypocotyl. 2,4-D inhibits apical hook, whereas relative low concentration of AAL1 does not (Fig. 1). This difference is verified by *ecr1-2*, whose aggravated apical hook could be inhibited by 2,4-D rather than AAL1 (Fig. 5a). Similar results were obtained from known auxin resistant mutant *axr1-3*, *af6/8* and *arf17* (Supplemental Fig. S5a, S9b). The exaggerated apical hook of *ecr1-2* is intriguing and similar to that of *ecr1-1* (Woodward et al. 2007). The exaggerated apical hook of *ecr1-2* could also be reduced by Ag^+ and AVG treatments (Fig. 5c), indicating that the exaggerated apical hook depends on ethylene pathway. It was reported that auxin could activate ethylene pathway through ethylene biosynthesis and signaling (Thomann et al. 2009; Woodward et al. 2007). The mechanism how AAL1 aggravates the apical hook of some auxin related mutants is unclear. One possibility is that the effect of AAL1 is too weak to inhibit the exaggerated apical

hook caused by activated ethylene pathway. Consistently, extremely high concentration of AAL1 could also inhibit apical hook (Supplemental Fig. S1). As apical hook can be caused by the asymmetric distribution of auxin (Muday and Murphy 2002), another possibility is that AAL1 could not be efficiently transported to the apical hook to counterbalance the asymmetric distribution of auxin.

Like other known auxins, AAL1 functions depending on auxin transporters, such as AUX1. Six AAL1 resistant *aux1* alleles identified in this study support this notion. Three *aux1* missense mutants *aux1-87aa*, *aux1-143aa*, *aux1-467aa* identified in this study were mapped to new positions of AUX1 protein (Supplemental Fig. S11) (Swarup et al. 2004). Major auxin influx carriers AUX1/LAXs belong to the amino acid permease family (Bennett et al. 1996; Swarup et al. 2008). Amino acid transporter ANT1 could transport Tyr, Phe, Trp, IAA and 2,4-D (Chen et al. 2001).

The third difference between AAL1 and known auxinic compounds is its relationship with some amino acids. Our results showed that certain amino acids such as Tyr and Phe could reduce the inhibitory effects of AAL1 (Fig. 7). It is plausible that specific amino acids can affect auxin action by competing auxin transporter AUX1. This is supported by the observation that *aux1-196aa* and *aux1-439aa* showed weak resistance to Phe (Supplemental Fig. S13g). Previous reports also showed that some amino acids could be conjugated to IAA (Staswick et al. 2005). If so, free levels of AAL1 and IAA will be reduced when co-treated with these amino acids. This hypothesis is supported by previous observation that *trp5* accumulates soluble Trp about threefold higher than that in wild-type and is resistant to IAA (Staswick 2009). We also found that adding Trp could reduce the inhibitory effects of IAA and the effects of IAA and 2,4-D/AAL1 could be obviously inhibited by Trp and Tyr respectively (Fig. 7, Supplemental Fig. S13). It seems that specific amino acid could conjugate auxin with similar structure, for example Trp conjugates IAA, Tyr/Phe conjugates 2,4-D/AAL1 (Staswick 2009). Apart from being precursor of auxin, amino acids may affect auxin pathway via other pathways such as cellular metabolisms. Thus application of Auxin-like chemicals such as AAL1 may provide useful tools for studying weak functions of amino acids in auxin pathway.

Materials and methods

Plant material and growth condition

All the plants used in this research were *Arabidopsis thaliana* accession Col-0 unless otherwise indicated. The *axr2-1* (CS3077), *axr1-3* (CS3075), *tir1-1* (CS3798), *yuc1/2/4/6* mutants and *DR5::GUS* transgenic lines were gifts from

laboratories of Dr. Hai Huang, Dr. Lin Xu and Dr. Zuhua He in Shanghai Institute of Plant Physiology and Ecology (SIPPE).

For chemical treatment assays, seeds were grown on 0.5×MS solid medium in continuous dark for 3 days as described (Zhao et al. 2007). For seeds harvest and shoot phenotype analysis, plants were grown in long-day condition at 22 °C.

Phenotype-based chemical genetics screening

The plant chemical genetics screenings were performed as the ones previously described, the plants grown on 0.5×MS solid medium containing 1% DMSO were used as blank controls (Ye et al. 2016; Li et al. 2017).

Hyposensitive mutants screening and map-based cloning

The plant chemical genetics phenotypes were observed and imaged using a SZX16 dissecting microscope (Olympus) and the length of *Arabidopsis* hypocotyls or roots were measured using Image J (NIH).

Ethyl methane sulfonate (EMS) mutagenized *Arabidopsis* M2 mutant seeds were sown on 0.5×MS solid medium with 100 μM AAL1 and grew for 3 days in the continuous dark condition at 22 °C, seedlings with longer root or hypocotyl were acquired, and retested and genetically analyzed in the next generations. Mutant genes responsible for AAL1 resistant phenotypes of the mutants were identified by the map-based cloning using the chemical genetic phenotypes of the mutants combined with molecular marks from the *Arabidopsis* Mapping Platform (Hou et al. 2010), followed with genomic DNA sequence analysis. For each isolated mutants showed auxin-associated phenotypes, more than 200 F2 seedlings with the specific chemical genetics phenotype were used to map gene.

Complement assay for *ecr1-2*

The transgenic constructs and plant transformation experiments were performed as previously described (Ye et al. 2016). The promoter and coding sequences of ECR1 (AT5G19180) were amplified by PCR from genomic DNA and cDNA of Col-0. Using primers are listed in Table S1.

Quantitative real-time RT-PCR (qRT-PCR)

The qRT-PCRs were accomplished as previously described (Ye et al. 2016). 3-day-old dark-grown Col-0 seedlings were collected and dipped in 0.5×MS media with 50 μM AAL1, 10 μM IAA or 1% DMSO for 0.5 h or 3 h. Total RNAs were extracted and used to synthesize the cDNAs by reverse

transcription. All primers used were listed in Table S1. The *ACTIN* gene was amplified and used as an internal control.

Confocal observation and imaging

6-day-old light-grown DII-VENUS transgenic seedlings were transferred to media with 100 μM AAL1, 5 μM IAA, 0.5 μM 2,4-D or 1% DMSO for 0.5 h or 3 h. The fluorescence signal was observed and imaged under a confocal microscope (Olympus FV1000). Data quantification of the microscope images was performed using ImageJ (Yokawa et al. 2016).

The molecular docking of AAL1 with TIR1-IAA7 complex

Molecular docking was done as described previous (Narukawa-Nara et al. 2016; Mageroy et al. 2015; Katz et al. 2015). The 3D structure of chemicals in SDF format taken from the National Center for Biotechnology Information PubChem server (<http://www.ncbi.nlm.nih.gov/>) was converted into PDB format via the Molecular formats converter server (<http://www.webqc.org/molecularformatsconverter.php>). Structure of TIR1-IAA7 complex in PDB format (PDB ID 2P1Q) taken from RCSB Protein Data Bank (<http://www.rcsb.org/pdb/home/home.do>) was prepared by Dock Prep tool of Chimera-1.11.2 software.

The molecule docking of AAL1 with TIR1-IAA7 complex was then performed with the software AutoDock4.2 (<http://autodock.scripps.edu>). Automated docking was used to locate the appropriate binding orientations and conformations of TIR1 in the auxin binding pocket. To perform the task, genetic algorithm routine implemented in the program AutoDock 4.2 was employed. The program AutoGrid was used to generate the grid maps that represent the intact ligand in the actual docking target site. A grid box was used to prepare a grid map with a size of $60 \times 60 \times 60$ Å xyz points. The grid center was designated at dimensions (x, y, z): 6.2454,-116.05956,-28.69364. The standard docking protocol for rigid and flexible ligand docking consisted of 10 independent runs per ligand. After docking, 10 models were calculated, and the one with the lowest binding energy was chosen for further energy minimization. 3D and 2D docking results were visualized by Chimera-1.11.2 and LigPlot + v.1.4 respectively.

LC-MS Analysis of AAL1 treated seedlings

AAL1 standard is 50 ng/ μL and dissolved in acetonitrile. Seeds were imbibed on solid medium with 100 μM AAL1 at 4 °C for 3 days and germinated for 3 days at 22 °C in darkness. About 300 mg seedlings were collected and subsequently grinded by liquid nitrogen and incubated with

acetonitrile. The extracts were clarified by centrifugation. LC-MS analysis was performed as the ones previously described (Zhao et al. 2007).

Acknowledgements We thank Dr. Xiaoya Chen (SIPPE) and Dr. Yongfei Wang for providing the Col-0 EMS mutant M2 seeds. We also thank Dr. Zuhua He (SIPPE), Hai Huang (SIPPE) and Lin Xu (SIPPE) for providing auxin-associated mutants. This work was supported by grants from the National Natural Science Foundation of China (31171293 and 31371361) and the One Hundred Talents grant of the Chinese Academy of Sciences to Yang Zhao, and the National Natural Science Foundation of China (31630014) and the Strategic Priority Program of Chinese Academy of Sciences (XDB27020104) to Laigeng Li.

Author Contributions YZ and WBL planned and designed the research. WBL and HML performed experiments, conducted fieldwork, analyzed data and wrote the manuscript. LTL helped to perform experiments. YZ, LGL and YJZ modified the manuscript. PX, DQL, YJY and ZX helped to modify the manuscript. YJZ and LGL provided platform for some experiments.

Compliance with ethical standards

Conflict of interest The authors declare that they have no conflict of interest.

References

- Bennett MJ, Marchant A, Green HG, May ST, Ward SP, Millner PA, Walker AR, Schulz B, Feldmann KA (1996) Arabidopsis AUX1 gene: A permease-like regulator of root gravitropism. *Science* 273(5277):948–950
- Cao M, Liu X, Zhang Y, Xue X, Zhou XE, Melcher K, Gao P, Wang F, Zeng L, Zhao Y, Zhao Y, Deng P, Zhong D, Zhu JK, Xu HE, Xu Y (2013) An ABA-mimicking ligand that reduces water loss and promotes drought resistance in plants. *Cell Res* 23(8):1043–1054
- Chen LS, Ortiz-Lopez A, Jung A, Bush DR (2001) ANT1, an aromatic and neutral amino acid transporter in Arabidopsis. *Plant Physiol* 125(4):1813–1820
- Cheng YF, Dai XH, Zhao YD (2004) AtCAND1, a HEAT-repeat protein that participates in auxin signaling in Arabidopsis. *Plant Physiol* 135(2):1020–1026
- Cheng YF, Dai XH, Zhao YD (2006) Auxin biosynthesis by the YUCCA flavin monooxygenases controls the formation of floral organs and vascular tissues in Arabidopsis. *Genes Dev* 20(13):1790–1799
- Dai XH, Hayashi K, Nozaki H, Cheng YF, Zhao YD (2005) Genetic and chemical analyses of the action mechanisms of sirtinol in Arabidopsis. *Proc Natl Acad Sci USA* 102(8):3129–3134
- Del Pozo JC, Dharmasiri S, Hellmann H, Walker L, Gray WM, Estelle M (2002) AXR1-ECR1-dependent conjugation of RUB1 to the Arabidopsis cullin AtCUL1 is required for auxin response. *Plant Cell* 14(2):421–433
- Enders TA, Strader LC (2015) Auxin activity: past, present, and future. *Am J Bot* 102(2):180–196
- Estelle M (1998) Polar auxin transport: new support for an old model. *Plant Cell* 10(11):1775–1778
- Grossmann K (2007) Auxin herbicide action: lifting the veil step by step. *Plant Signal Behav* 2(5):421–423
- Hosek P, Kubes M, Lanková M, Dobrev PI, Klíma P, Kohoutová M, Petrášek J, Hoyerová K, Jirina M, Zazimalová E (2012) Auxin

- transport at cellular level: new insights supported by mathematical modelling. *J Exp Bot* 63(10):3815–3827
- Hou X, Li L, Peng Z, Wei B, Tang S, Ding M, Liu J, Zhang F, Zhao Y, Gu H, Qu LJ (2010) A platform of high-density INDEL/CAPS markers for map-based cloning in *Arabidopsis*. *Plant J* 63(5):880–888
- Katz E, Nisani S, Yadav BS, Woldemariam MG, Shai B, Obolski U, Ehrlich M, Shani E, Jander G, Chamovitz DA (2015) The glucosinolate breakdown product indole-3-carbinol acts as an auxin antagonist in roots of *Arabidopsis thaliana*. *Plant J* 82(4):547–555
- Kazan K (2013) Auxin and the integration of environmental signals into plant root development. *Ann Bot* 112(9):1655–1665
- Kepinski S, Leyser O (2005) The *Arabidopsis* F-box protein TIR1 is an auxin receptor. *Nature* 435(7041):446–451
- Lavy M, Prigge MJ, Tao S, Shain S, Kuo A, Kirchsteiger K, Estelle M (2016) Constitutive auxin response in *Physcomitrella* reveals complex interactions between Aux/IAA and ARF proteins. *Elife* 5:e13325
- Leyser HMO, Lincoln CA, Timpte C, Lammer D, Turner J, Estelle M (1993) *Arabidopsis* auxin-resistance gene-Auxr1 encodes a protein related to Ubiquitin-activating enzyme-E1. *Nature* 364(6433):161–164
- Li SB, Xie ZZ, Hu CG, Zhang JZ (2016) A review of auxin response factors (ARFs) in plants. *Front Plant Sci* 7:47
- Li W, Lacey RF, Ye Y et al (2017) Triplin, a small molecule, reveals copper ion transport in ethylene signaling from ATX1 to RAN1. *PLoS Genet* 13(4):e1006703
- Liu X, Zhang H, Zhao Y, Feng Z, Li Q, Yang HQ, Luan S, Li J, He ZH (2013) Auxin controls seed dormancy through stimulation of abscisic acid signaling by inducing ARF-mediated ABI3 activation in *Arabidopsis*. *Proc Natl Acad Sci USA* 110(38):15485–15490
- Liu Y, Xu M, Liang N, Zheng Y, Yu Q, Wu S (2017) Symplastic communication spatially directs local auxin biosynthesis to maintain root stem cell niche in *Arabidopsis*. *Proc Natl Acad Sci USA* 114(15):4005–4010
- Ma Q, Robert S (2014) Auxin biology revealed by small molecules. *Physiol Plant* 151(1):25–42
- Mageroy MH, Parent G, Germanos G, Giguère I, Delvas N, Maaroufi H, Bauce É, Bohlmann J, Mackay JJ (2015) Expression of the beta-glucosidase gene Pg beta glu-1 underpins natural resistance of white spruce against spruce budworm. *Plant J* 81(1):68–80
- Marchant A, Kargul J, May ST, Muller P, Delbarre A, Perrot-Rechenmann C, Bennett MJ (1999) AUX1 regulates root gravitropism in *Arabidopsis* by facilitating auxin uptake within root apical tissues. *Embo J* 18(8):2066–2073
- McCourt P, Desveaux D (2010) Plant chemical genetics. *New Phytol* 185(1):15–26
- Meesters C, Mönig T, Oeljeklaus J, Krahn D, Westfall CS, Hause B, Jez JM, Kaiser M, Kombrink E (2014) A chemical inhibitor of jasmonate signaling targets JAR1 in *Arabidopsis thaliana*. *Nat Chem Biol* 10:830–836
- Muday GK, Murphy AS (2002) An emerging model of auxin transport regulation. *Plant Cell* 14(2):293–299
- Nagpal P, Walker LM, Young JC, Sonawala A, Timpte C, Estelle M, Reed JW (2000) AXR2 encodes a member of the Aux/IAA protein family. *Plant Physiol* 123(2):563–574
- Narukawa-Nara M, Nakamura A, Kikuzato K, Kakei Y, Sato A, Mitani Y, Yamasaki-Kokudo Y, Ishii T, Hayashi K, Asami T, Ogura T, Yoshida S, Fujioka S, Kamakura T, Kawatsu T, Tachikawa M, Soeno K, Shimada Y (2016) Aminoxy-naphthylpropionic acid and its derivatives are inhibitors of auxin biosynthesis targeting l-tryptophan aminotransferase: structure-activity relationships. *Plant J* 87(3):245–257
- Okushima Y, Overvoorde PJ, Arima K, Alonso JM, Chan A, Chang C, Ecker JR, Hughes B, Lui A, Nguyen D, Onodera C, Quach H, Smith A, Yu G, Theologis A (2005) Functional genomic analysis of the AUXIN RESPONSE FACTOR gene family members in *Arabidopsis thaliana*: unique and overlapping functions of ARF7 and ARF19. *Plant Cell* 17(2):444–463
- Ouellet F, Overvoorde PJ, Theologis A (2001) IAA17/AXR3: biochemical insight into an auxin mutant phenotype. *Plant Cell* 13(4):829–841
- Park SY, Fung P, Nishimura N, Jensen DR, Fujii H, Zhao Y, Lumba S, Santiago J, Rodrigues A, Chow TF, Alfred SE, Bonetta D, Finkelstein R, Provart NJ, Desveaux D, Rodriguez PL, McCourt P, Zhu JK, Schroeder JI, Volkman BF, Cutler SR (2009) Abscisic acid inhibits type 2C protein phosphatases via the PYR/PYL family of START proteins. *Science* 324(5930):1068–1071
- Peer WA, Blakeslee JJ, Yang HB, Murphy AS (2011) Seven things we think we know about auxin transport. *Mol Plant* 4(3):487–504
- Reed JW (2001) Roles and activities of Aux/IAA proteins in *Arabidopsis*. *Trends Plant Sci* 6(9):420–425
- Rouse D, Mackay P, Stürnberg P, Estelle M, Leyser O (1998) Changes in auxin response from mutations in an AUX/IAA gene. *Science* 279(5355):1371–1373
- Ruegger M, Dewey E, Gray WM, Hobbie L, Turner J, Estelle M (1998) The TIR1 protein of *Arabidopsis* functions in auxin response and is related to human SKP2 and yeast Grr1p. *Genes Dev* 12(2):198–207
- Simon S, Kubes M, Baster P, Robert S, Dobrev PI, Friml J, Petrášek J, Zažímalová E (2013) Defining the selectivity of processes along the auxin response chain: a study using auxin analogues. *New Phytol* 200(4):1034–1048
- Soeno K, Goda H, Ishii T, Ogura T, Tachikawa T, Sasaki E, Yoshida S, Fujioka S, Asami T, Shimada Y (2010) Auxin biosynthesis inhibitors, identified by a genomics-based approach, provide insights into auxin biosynthesis. *Plant Cell Physiol* 51:524–536
- Spyropoulos IC, Liakopoulos TD, Bagos PG, Hamodrakas SJ (2004) TMRPres2D: high quality visual representation of transmembrane protein models. *Bioinformatics* 20(17):3258–3260
- Staswick PE (2009) The tryptophan conjugates of jasmonic and indole-3-acetic acids are endogenous auxin inhibitors. *Plant Physiol* 150(3):1310–1321
- Staswick PE, Serban B, Rowe M, Tiryaki I, Maldonado MT, Maldonado MC, Suza W (2005) Characterization of an *Arabidopsis* enzyme family that conjugates amino acids to indole-3-acetic acid. *Plant Cell* 17(2):616–627
- Strader LC, Beisner ER, Bartel B (2009) Silver ions increase auxin efflux independently of effects on ethylene response. *The Plant cell* 21:3585–3590
- Swarup R, Kargul J, Marchant A, Zadik D, Rahman A, Mills R, Yemm A, May S, Williams L, Millner P, Tsurumi S, Moore I, Napier R, Kerr ID, Bennett MJ (2004) Structure-function analysis of the presumptive *Arabidopsis* auxin permease AUX1. *Plant Cell* 16(11):3069–3083
- Swarup K, Benková E, Swarup R, Casimiro I, Péret B, Yang Y, Parry G, Nielsen E, De Smet I, Vanneste S, Levesque MP, Carrier D, James N, Calvo V, Ljung K, Kramer E, Roberts R, Graham N, Marillonnet S, Patel K, Jones JD, Taylor CG, Schachtman DP, May S, Sandberg G, Benfey P, Friml J, Kerr I, Beeckman T, Laplace L, Bennett MJ (2008) The auxin influx carrier LAX3 promotes lateral root emergence. *Nat Cell Biol* 10(8):946–954
- Tan X, Calderon-Villalobos LI, Sharon M, Zheng C, Robinson CV, Estelle M, Zheng N (2007) Mechanism of auxin perception by the TIR1 UBIQUITIN ligase. *Nature* 446(7136):640–645
- Teale WD, Paponov IA, Palme K (2006) Auxin in action: signalling, transport and the control of plant growth and development. *Nat Rev Mol Cell Biol* 7(11):847–859
- Thomann A, Lechner E, Hansen M, Dumbliuskas E, Parmentier Y, Kieber J, Scheres B, Genschik P (2009) *Arabidopsis* CULLIN3 genes regulate primary root growth and patterning by

- ethylene-dependent and -independent mechanisms. *PLoS Genet* 5(1):e1000328
- Tian Q, Reed JW (1999) Control of auxin-regulated root development by the *Arabidopsis thaliana* SHY2/IAA3 gene. *Development* 126(4):711–721
- Tian Q, Uhlir NJ, Reed JW (2002) *Arabidopsis* SHY2/IAA3 inhibits auxin-regulated gene expression. *Plant Cell* 14(2):301–319
- Tusnady GE, Simon I (2001) The HMMTOP transmembrane topology prediction server. *Bioinformatics* 17(9):849–850
- Villalobos LIaC, Lee S, De Oliveira C et al (2012) A combinatorial TIR1/AFB-Aux/IAA co-receptor system for differential sensing of auxin. *Nat Chem Biol* 8(5):477–485
- Walsh TA, Neal R, Merlo AO, Honma M, Hicks GR, Wolff K, Matsumura W, Davies JP (2006) Mutations in an auxin receptor homolog AFB5 and in SGT1b confer resistance to synthetic picolinate auxins and not to 2,4-dichlorophenoxyacetic acid or indole-3-acetic acid in *Arabidopsis*. *Plant Physiol* 142(2):542–545
- Woodward AW, Ratzel SE, Woodward EE, Shammoo Y, Bartel B (2007) Mutation of E1-conjugating enzyme-related1 decreases related to Ubiquitin conjugation and alters auxin response and development. *Plant Physiol* 144(2):976–987
- Yang YD, Hammes UZ, Taylor CG, Schachtman DP, Nielsen E (2006) High-affinity auxin transport by the AUX1 influx carrier protein. *Curr Biol* 16(11):1123–1127
- Ye Y, Gong Z, Lu X, Miao D, Shi J, Lu J, Zhao Y (2016) Germostatin resistance locus 1 encodes a PHD finger protein involved in auxin-mediated seed dormancy and germination. *Plant J* 85(1):3–15
- Ye Y, Zhou L, Liu X et al (2017) A novel chemical inhibitor of ABA signaling targets all ABA receptors. *Plant Physiol* 173(4):2356–2369
- Yokawa K, Kaquenishi T, Baluska F (2016) UV-B induced generation of reactive oxygen species promotes formation of BFA-induced compartments in cells of *Arabidopsis* root apices. *Front Plant Sci* 6:1162
- Zhao YD (2010) Auxin biosynthesis and its role in plant development. *Annu Rev Plant Biol* 61:49–64
- Zhao YD, Dai XH, Blackwell HE, Schreiber SL, Chory J (2003) SIR1, an upstream component in auxin signaling pathway identified by chemical genetics. *Science* 301(5636):1107–1110
- Zhao Y, Chow TF, Puckrin RS et al (2007) Chemical genetic interrogation of natural variation uncovers a molecule that is glycoactivated. *Nat Chem Biol* 3(11):716–721
- Zolman BK, Bartel B (2004) An *Arabidopsis* indole-3-butyric acid-response mutant defective in PEROXIN6, an apparent ATPase implicated in peroxisomal function. *Proc Natl Acad Sci USA* 101(6):1786–1791
- Zolman BK, Yoder A, Bartel B (2000) Genetic analysis of indole-3-butyric acid responses in *Arabidopsis thaliana* reveals four mutant classes. *Genetics* 156(3):1323–1337
- Zolman BK, Martinez N, Millius A, Adham AR, Bartel B (2008) Identification and characterization of *Arabidopsis* indole-3-butyric acid response mutants defective in novel peroxisomal enzymes. *Genetics* 180(1):237–251